Satellite and modelling based snow season time series for Svalbard: Inter-comparisons and assessment of accuracy (SATMODSNOW)

Eirik Malnes[1], Hannah Vickers[1], Stein Rune Karlsen[1], Tuomo Saloranta[2], Mari Anne Killie[3], Ward Van Pelt[4], Veijo Pohjola[4], Jie Zhang[4], Laura Stendardi[5], and Claudia Notarnicola[5]

1 NORCE Norwegian Research Centre, Bergen, Norway
2 The Norwegian Water Resources and Energy Directorate (NVE), 0368 Oslo, Norway
3 The Norwegian Meteorological Institute, 0371 Oslo, Norway
4 Department of Earth Sciences, Uppsala University, Uppsala, Sweden
5 Eurac Research, Institute for Earth Observation, Bolzano, Italy

Corresponding author: Eirik Malnes, eima@norceresearch.no
ORCID number: 0000-0001-9824-9696

Keywords: Snow, remote sensing, modelling, snow cover, snow water equivalent

DOI: https://doi.org/10.5281/zenodo.4294072

1. Introduction

Consistent long-term datasets on snow cover and snow depth/snow water equivalent over Svalbard are scarce and affected by great uncertainties. Remote sensing provides a good platform for large-scale snow monitoring. Due to the scarcity of synoptic stations that measure snow (particularly before 2008) and lack of suitable satellite data, models of snow cover and associated parameters can be an alternative source of data. However, the reliability of snow models is often questionable since the input data used are predominantly based on modelling assumptions and large-scale numerical reanalysis. In this study, currently available models are reviewed and snow model products are compared with remote sensing datasets by evaluating their overall performance for the part of Svalbard where seasonal snow exists.

The following objectives are specifically addressed:

- To identify years/periods where models and Earth Observation (EO) datasets differ significantly
- To identify areas where models and EO datasets differ significantly
- To cross-compare EO datasets at variable scales (AVHRR, MODIS, Sentinel-2) and suggest methods for how newer high-resolution data can be used in combination with moderate or low-resolution data to construct high resolution and long timeseries datasets by making corrections to earlier datasets based on their sensor resolution bias

2. Overview of existing knowledge

This section gives an overview of the datasets used in this study with emphasis on the periglacial landscape in Svalbard (i.e., the non-glaciated land in Svalbard where seasonal snow exists). Table 1 provides an overview of all datasets used in this project. Table 2 contains more information on the details in the different datasets used.

2.1. Satellite data

Remote sensing satellite data have been available since 1978. The earliest satellites generally had coarse resolution except for Landsat.

2.1.1. MODIS

Optical data from the Moderate Resolution Imaging Spectroradiometer (MODIS) onboard Terra and Aqua satellites have been available since 2000. A 20-year snow cover fraction dataset for Svalbard based on the NASA MOD10A1-product (Hall et al., 2002) from the MODIS Terra satellite has been described by Vickers et al. (2020). The MOD10A1-product uses the spectral band 4 (visible light) and band 6 (short wave infrared) to estimate the normalized differential snow index (NDSI) defined by the relation $NDSI = (band4 - band6) / (band4 + band6)$. The snow cover fraction (SCF) as a percentage is then estimated using the relation $SCF = (0.06 + 1.21NDSI) \times 100$. In addition, cloud cover is detected and masked out. In Svalbard, the polar night period is present from mid-October to mid-February. Since MODIS is an optical sensor, there is no data coverage during the dark period and the MOD10A1 product is only provided from March 1 to November 1. During the polar night, SCF is set to 100 %. The NORCE-derived product provides SCF for the entire periglacial landscape in Svalbard as a temporally interpolated product at daily intervals and 500 m resolution. This is a compromise between the 250 m resolution for the visual channels of MODIS, and the infra-red channel used for cloud discrimination. Since MODIS has moderate spatial resolution and excellent temporal overlap with the other satellite and modelled data products in this study, the MODIS dataset is used throughout this SESS report as a baseline for comparisons.

2.1.2. AVHRR

The Advanced Very High Resolution Radiometer (AVHRR) instrument has flown onboard polar orbiting satellites since the late 1970s. The instrument has approximately 1 km resolution, but only data at a reduced effective resolution of approximately 4 km is permanently archived and available with global coverage. From the AVHRR Global Area Coverage (GAC) data, a fundamental climate data record (FCDR) for radiances and brightness temperatures has been made available by the EUMETSAT Climate Monitoring Satellite Application Facility (CM SAF). The current release 'CLARA-A2' covers 1982–2015 (Karlsson et al., 2017).

Using the probabilistic snow cover algorithm provided by MET Norway, a time series of daily snow cover maps covering the Svalbard archipelago at 4 km grid spacing has been derived from the CLARA-A2 FCDR. The snow cover algorithm uses a set of signatures (instrument channel combinations) and statistical coefficients. The latter are derived from prior knowledge of the typical behaviour of the surface classes across the spectrum. Cloud-free pixels from the AVHRR GAC swath products are averaged and gridded to produce daily maps of average snow probability. A threshold of 50 % is applied to the snow probability maps to derive a binary snow/no snow product. Since the algorithm uses satellite measurements of reflected sunlight, there will be areas of no data due to winter darkness, therefore limiting data coverage between March 1 and September 30 each year. Therefore, the melting season is well covered, but the onset of the snow season is concealed due to the onset of the polar night period. In addition, temporal gap filling has been applied to achieve daily cloud-free mosaics.

2.1.3. Sentinel-2/Landsat-8

The Sentinel-2 (S2) A and B satellites have been delivering data over Svalbard since spring 2016 (Sentinel-2 User guide). The instrument provides data with nominal 10 m pixel spacing and is very well suited for snow cover mapping under cloud-free conditions. Since the launch of the Sentinel-2B satellite in 2017, daily coverage of Svalbard has been possible. Furthermore, the Landsat-8 satellite has comparable spatial resolution (30 m) and was launched in 2014, thereby extending the period with high-resolution data coverage. Prior to this, only a few datasets for Svalbard were available, provided by Landsat-5 and Landsat-7 satellites.

In this report, we use a time-series of S2 NDSI products interpolated in the temporal dimension between cloud free observations. For the NDSI, we derive the SCF using the same relation as for MODIS (section 2.1.1). We thus obtain daily cloud free SCF-maps with 10 m resolution that can be directly compared with the MODIS dataset. Only the years 2018 and 2019 were available to use in this study.

2.1.4. Other remote sensing datasets

A range of microwave sensors can also be used for remote sensing of snow. Passive microwave sensors such as the Special Sensor Microwave/Imager (SSM/I) have provided decadal-long time series of snow water equivalent (SWE) estimates (e.g. Pulliainen et al., 2020), but the very coarse spatial resolution (~10-20 km) and lack of sensitivity over mountainous areas make these sensors less suitable for Svalbard, which is dominated by mountainous topography.

Microwave scatterometers have somewhat better resolution (~5km) and have also been used to some extent for studies in Svalbard. Rotschky et al. (2011) studied the spatio-temporal variability of snowmelt in Svalbard during 2000–2008 using QuikSCAT. A drawback associated with using active microwave sensors is their poor ability to distinguish between dry snow and bare soil. The main detection method for snowmelt is based on the high contrast between wet snow and dry snow/bare soil, which can also be applied to Synthetic aperture radar (SAR) data to quantify wet snow events (Nagler and Rott, 2000). In the current SIOS project, NORCE is adapting a time series of Envisat ASAR, Radarsat-2 and Sentinel-1 (S1) images over Svalbard to produce wet snow maps for the period 2002–2020. Stendardi (2020, PhD dissertation) has also studied the detailed melting patterns in

Adventdalen using combinations of S1 and S2. Similar studies of the freeze/thaw conditions on Kapp Linne have been published by Eckerstorfer et al. (2020). Multi-sensor approaches which combined optical and SAR data were also studied by Malnes et al. (2010).

ESA CCI Snow will provide global datasets for snow extent and SWE (1979–2018)12'global' snow extent service provides daily data over continental Europe at 500m spatial resolution but excludes Svalbard and is hence not relevant. A high-resolution Fractional Snow Cover product has recently been made available by Copernicus based on Sentinel-2[3] This product will, however, only cover areas up to 66°N and is therefore also unfortunately irrelevant for Svalbard (Gascoin et al., 2019).

2.2. Snow models

Snow models can simulate the evolution of relevant snow parameters continuously in space and time and are therefore an important tool to fill spatial and temporal gaps in observational datasets and simulate snow over longer time-periods and larger spatial domains. They require a surface meteorological forcing, which may come from regional climate model output or reanalysis datasets for large-scale modelling. Seasonal snowpack evolution on land areas in Svalbard is dominated by snow accumulation during autumn and winter and subsequent melting during late spring and summer. While cumulative snow accumulation and spring maximum snow depth is mostly determined by cumulative precipitation (snowfall) in autumn and winter, snow melt depends on atmosphere-surface interactions and can be estimated using simple melt-air temperature relationships (positive-degree day model) or more sophisticated models that solve the surface energy balance. Subsurface models may vary in terms of complexity but typically track at least the evolution of subsurface density, temperature and water content. In situ and/or remote sensing snow products (e.g. SWE, snow depth, density, temperature and water content) are essential for model calibration and validation.

2.2.1. SeNorge

Up-to-date information on snow conditions is a crucial element for forecasting of natural hazards such as avalanches, slush flows and snow melt floods. Operational daily maps of simulated snow conditions have already existed for 15 years for mainland Norway[4]. However, no such detailed and spatiotemporal information with good cover on snow conditions on Svalbard currently exists, despite the obvious relevance and need for such snow information in for example, natural hazard forecasting on Svalbard and planning of outdoor and tourism activities. Consequently, in a research and development project in 2019-2020 NVE endeavours to set up an operational numerical snow model for mapping snow conditions (snow depth, density and water equivalent, fraction of snow-covered area plus others) in Svalbard at 1x1 km resolution. The time series of simulated snow maps start in autumn 2012 and will be continuously updated until the present day, and even 2–3 days ahead from that in the short-term weather forecast period.

This study uses the seNorge snow model (Saloranta, 2016), which requires the 3-hourly or daily mean air temperature [°C] and the sum of precipitation [mm/3h] as its input forcing. The liquid and solid precipitation fractions are defined by a threshold air temperature (solid precipitation occurring if air temperature is ≤ 0.5 °C). The snow and ice melt are calculated using the extended degree-day model including air temperature and solar radiation terms. Subsequently, the two parameters of the melt algorithm have been estimated based on 3356 quality controlled daily melt rates observed by the Norwegian snow pillow network (Saloranta, 2014). The sub- grid snow distribution algorithm in the model (Saloranta, 2012) assumes that snow is distributed uniformly within the grid cells, i.e., all SWE values between a defined minimum and maximum value are equally likely within a grid cell. In addition, an even layer of new snow can form

1 http://snow-cci.enveo.at/
2 https://land.copernicus.eu/
3 https://land.copernicus.eu/pan-european/biophysical-parameters/high-resolution-snow-and-ice-monitoring
4 see www.senorge.no

on top of the uniformly distributed 'old' snowpack (SCA is then set to 1). The main effect of the sub-grid snow distribution is to reduce the grid cell average melting rates towards the late melt season rates when significant areas of bare ground are present in the grid.

The input data are aggregated from the hourly meteorological forcing data obtained and downscaled from the AROME Arctic numerical weather prediction model (NWP). Input precipitation in the current model application is scaled by a factor 0.75, based on initial evaluation of the first model results. The model parameter values are set to the same values as those in the application for mainland Norway, except the spatial snow distribution parameter CF is increased from the default value of 0.5 to 0.85, giving larger variance for sub-grid snow distribution. The model application for Svalbard starts at bare ground initial conditions in September 2012. Afterwards, snow/firn older than 1 year is removed from the model's snow store on 1st September each year. The two first snow seasons may thus be considered as a model 'spin-up' period at higher elevation areas with perennial snow.

The seNorge simulation data used and evaluated in this report are produced from the mid-term project version and updated and improved versions of the dataset may be produced during the ongoing project period until the end of 2020.

2.2.2. Snow modelling at Uppsala University (UU)

Using the snow modelling system SnowModel (Liston et al. 2006), Van Pelt et al. (2016) simulated the seasonal snowpack evolution across Svalbard at 1x1 km spatial resolution and a 3-hourly temporal resolution for 1957–2012. Driven by downscaled meteorological fields of precipitation, air temperature, relative humidity, wind speed and direction, and incoming shortwave and longwave radiation from the High Resolution Limited Area Model (HIRLAM; Reistad et al. 2009), SnowModel solves the surface energy balance and simulates the snow depth, density and temperature evolution. Precipitation was downscaled using an elevation relation, calibrated against a set of 1,442 SWE measurements collected on glaciers across Svalbard, to account for the effect of local topography on the precipitation distribution. For more details about the methods and dataset, the reader may referd to Van Pelt et al. (2016). The output of SWE is extracted from the model dataset and includes only seasonal snow, implying that multi-year (perennial) snow is excluded in this product.

A second snow model product has been extracted from a recent dataset of combined glacier climatic mass balance, seasonal snow and runoff, presented in Van Pelt et al. (2019). As such, driven by downscaled meteorological input from a regional climate model, a surface energy balance model calculates surface melt and temperature, and provides upper boundary conditions for a subsurface model, simulating the multi-layer evolution of snow density, temperature and water content (Van Pelt et al. 2012). More details on the model physics and calibration/validation can be found in Van Pelt et al. (2019). Here, SWE values are extracted from the model dataset and include both seasonal and multi-year snow. In this study, SWE derived from the 'older' (Van Pelt et al., 2016) SnowModel and the more recent, 'newer' (Van Pelt et al., 2019) SWE dataset described here are used in comparisons with the MODIS SCF products.

2.2.3. Other snow models

As part of the ongoing research and development at NVE, two other snow models are currently being run and evaluated in addition to the seNorge snow model. These are the single- and multi-layer snow schemes D95 and ISBA-ES of the land surface model SURFEX, which is part of the AROME NWP model system operated by the Norwegian Meteorological Institute (MET). The snow simulation results from D95 and ISBA-ES snow models are run with the same forcing data and spatial resolution as the seNorge model but are currently available only for the one-year period 1st September 2018–1st September 2019 due to higher computational requirements. The evaluation of the results from these two models will be described in the forthcoming final report from the project (expected to be published in early 2021).

2.3. Methods for comparison

2.3.1. Comparison of MODIS with AVHRR

The AVHRR 4 km gridded snow cover extent dataset uses the Lambert Azimuthal Equal Area projection. The two main products available are: 1) classed product corresponding to 5 classes (water, no data, snow-free pixels, snow-covered pixels, clouds) 2) gap-free classed product, a snow cover product corrected for cloud cover using information from cloud-free pixels up to 9 days forward or backward in time to correct for cloud-covered pixels in the present image and indicates whether the pixels are covered by snow or not together with the age of the reference image used to make the cloud cover corrections. This product gives in total 4 additional classes, with 3 classes each for both snow-free pixels and snow-covered pixels, and is used for the comparison as it allows a greater number of pixels to be used in the averaging of the AVHRR images.

The MODIS snow cover extent dataset uses a UTMZ33N projection at 500 m resolution. Therefore, the AVHRR dataset is re-projected to the MODIS grid before a comparison can be made. In addition, a vegetation map is used to mask out glaciers in the AVHRR dataset, as done to produce the MODIS SCF data (Vickers et al., 2020). In order to extract the snow cover fraction, the total number of snow-covered pixels in the AVHRR images are divided by the total number of remaining unmasked pixels in the image i.e., all pixels not classed as water, cloud, glacier or no data. Further, to extract the corresponding snow cover fraction from the MODIS images on the same day of year, the MODIS SCF is averaged over the same unmasked pixels as obtained from the AVHRR image. A 'land-averaged' snow cover extent/fraction product is therefore obtained for each day of year between March 1st and September 30th using the same pixels from both AVHRR and MODIS images.

2.3.2. Comparison of MODIS with Sentinel-2

A systematic comparison between MODIS and S2 for entire Svalbard is beyond the scope of the project, but a few direct comparisons have been done to assess the differences. Since S2 has 20m resolution and MODIS has 500m resolution, there is expected bias in the MODIS data when re-scaled to the same grid size as the S2 data. The same regression formula is used to calculate S2 SCF as was used for MODIS. The MODIS regression has been thoroughly validated, whereas the S2 regression to transform S2 NDSI to SCF is more uncertain. An example of snow cover maps obtained with S2 and MODIS for the Nordenskiöld Land region is presented in Figure 1. The regression between S2 and MODIS for the entire Nordenskiöld Land region has also been examined using the available 2-year dataset, but a longer time-series will be more advantageous.

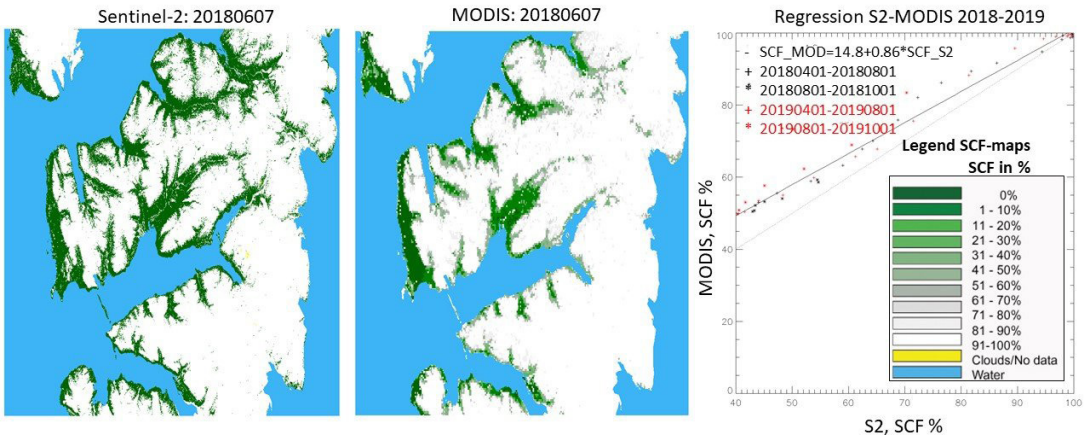

Figure 1: SCF-map for S2 (left) and MODIS (centre) for 20180607. Right: Regression between average SCF over Nordenskiöld Land for S2 and MODIS corresponding days in 2018 and 2019. Colours and symbols show differences between melting season (April–July) and fall (Aug–Nov).

2.3.3. Comparison of MODIS with SWE models (UU, NVE)

For the comparison of the two SWE datasets with the MODIS products, MODIS SCF maps were first georeferenced to the same grid as the SWE datasets. A glacier mask was also applied to the SWE data in the same way that the MODIS products have been masked. In order to obtain a comparable product, a threshold was applied to the SWE data such that pixels with a value below the threshold were classified as 'no snow' and those exceeding the threshold were considered snow covered. This allowed us to produce binary snow cover maps from the SWE data, from which an estimate of the land-averaged snow cover fraction could be derived, for each day of year in the time series. The optimal threshold was determined by trying 10 different thresholds on SWE ranging from 0.01 to 0.1 m and obtaining the land-averaged snow cover fraction time series resulting from the binary maps produced at each threshold. The difference between the SWE-derived SCF time series and the MODIS-derived SCF time series was calculated for each day of the year and the squared difference was summed over the whole year, for each year in the dataset. The threshold producing land-averaged SCF time series that gave the smallest squared-sum was identified as the best threshold for that year. Except for two years (2003 and 2004) where the optimal threshold was determined to be 0.02 m using the older dataset delivered by UU, the optimal threshold for the remainder of the dataset was found to be 0.01 m. Hence, the SWE-derived snow cover fraction time series obtained from the binary snow cover maps corresponding to a threshold of 0.01 m applied to the SWE data, were used to obtain the general relationship between the SWE and MODIS datasets.

Using the land-averaged snow cover fraction time series, the algorithm used to estimate the first snow free day (FSFD) from the MODIS dataset was applied to the SCF time series derived from the threshold SWE model maps. The same algorithm was also applied to the land averaged SCF time series produced using the re-gridded MODIS data. Note that this may not have necessarily produced the same results as for example, calculating the FSFD per pixel in the MODIS data and subsequently averaging all FSFD estimates over all land pixels.

2.3.4. Comparison of MODIS with seNorge snow-covered area

In addition to the SWE model provided by seNorge, snow-covered area (SCA) estimates were provided at 3-hour intervals on a daily basis for the years 2012–2019. This allowed an opportunity to directly compare SCF time series as well as SCA at a pixel level, after reprojecting the MODIS data to the same grid as the seNorge snow-covered area. SCA maps corresponding to 1200 UTC have been used to compare with the MODIS-derived SCF estimates.

2.3.5. Geographical comparison of snow cover

In the final part of the comparisons between the datasets, the difference in number of days with snow derived from each of the data products, compared with that obtained from MODIS is mapped. In order to make this geographical comparison, a binary snow map was created, in the case of the SWE datasets by thresholding at 0.01 cm and for MODIS SCF, by thresholding at 50%. Since the AVHRR maps already represented a binary snow cover extent, adapting this product was not needed. Hence, for each pixel in the grid, the number of days in a year the pixel was classified as snow covered/not snow covered during each year using the AVHRR, MODIS and SWE datasets was calculated. The difference in number of days with snow cover between AVHRR and MODIS, and the SWE datasets and MODIS was then calculated at each pixel.

3. Results

For the comparison of land-averaged SCF derived from AVHRR snow cover extent maps, the AVHRR SCF estimates were found to be systematically greater than MODIS SCF for all years studied, as shown by the time series plots in Figure 2 and the scatter plot comparison for the general relationship for these land averaged SCF estimates shown in Figure 3. The relationship was nonlinear, with differences of up to 30 %. For the lowest and highest SCF the two methods tended to converge.

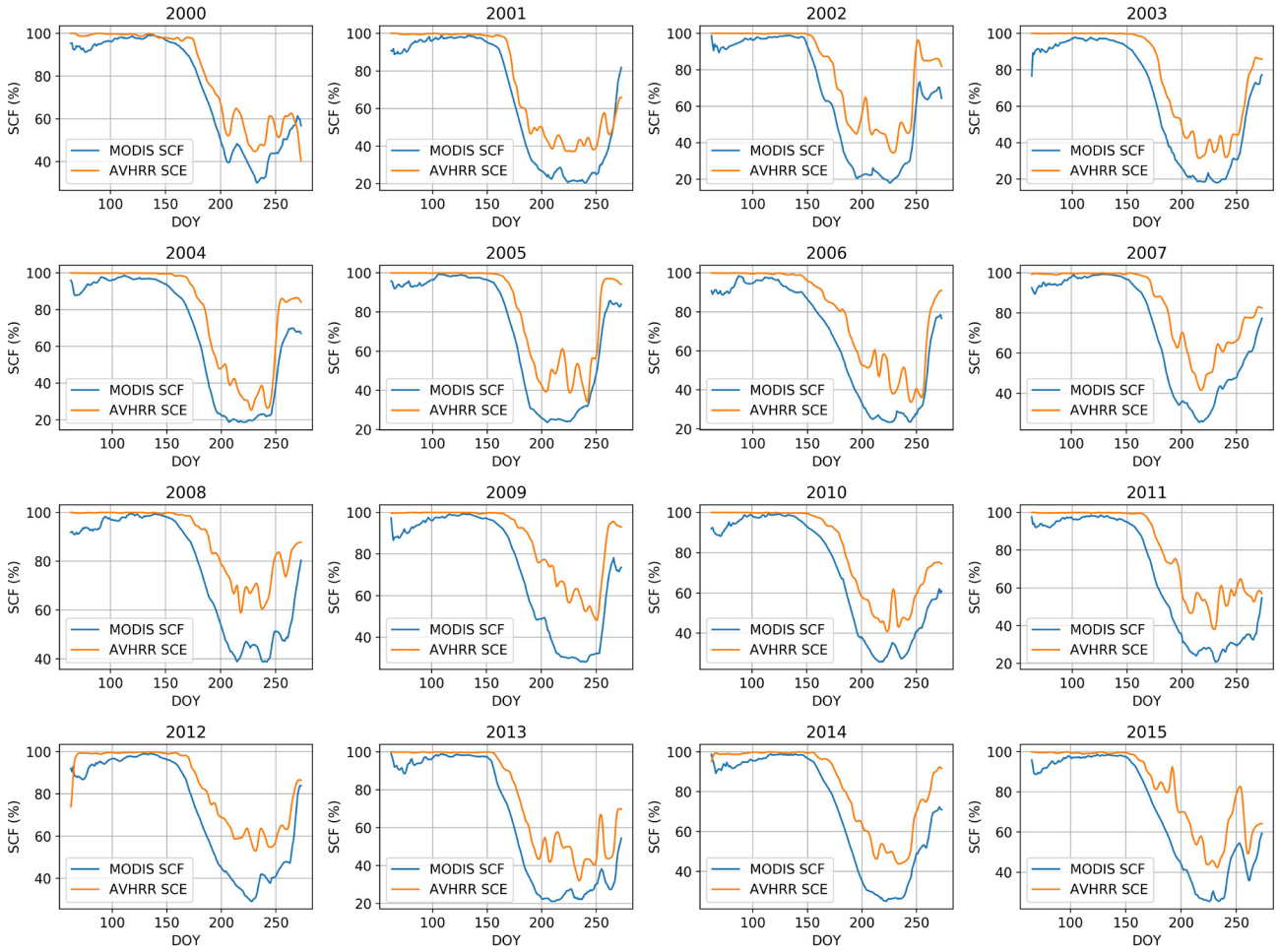

Figure 2: Comparison of SCF time series from AVHRR (orange) and MODIS (blue) for 2000–2015, using the maximum cloud-free gap of 9 days to select AVHRR data.

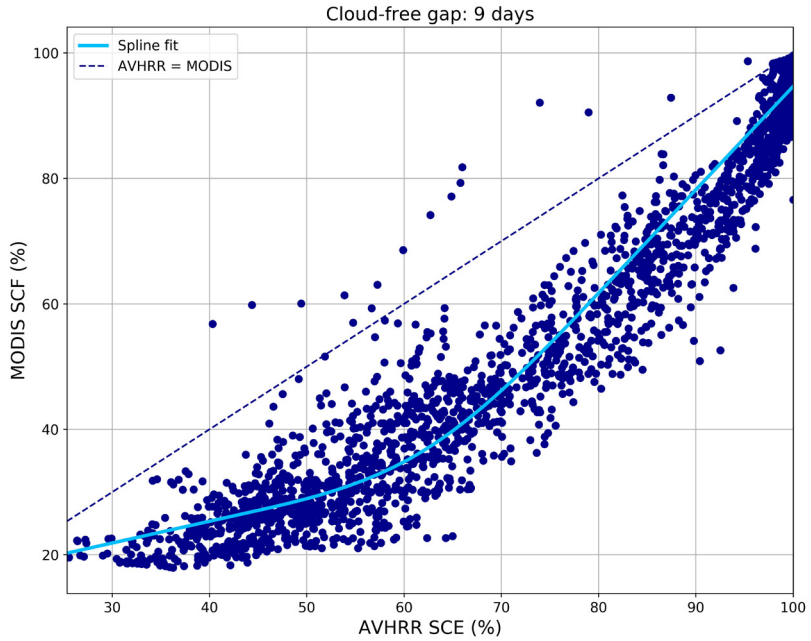

Figure 3: Comparison of SCF from AVHRR and MODIS as a scatter plot, combining the land-averaged estimates from all days of the year and all years (2000–2015), using the maximum cloud-free gap of 9 days. A fitted spline curve is shown in light blue and a dashed line indicates where the land-averaged estimates from both sensors would be equal, implying that in this case, the MODIS SCF is consistently lower than those derived from AVHRR.

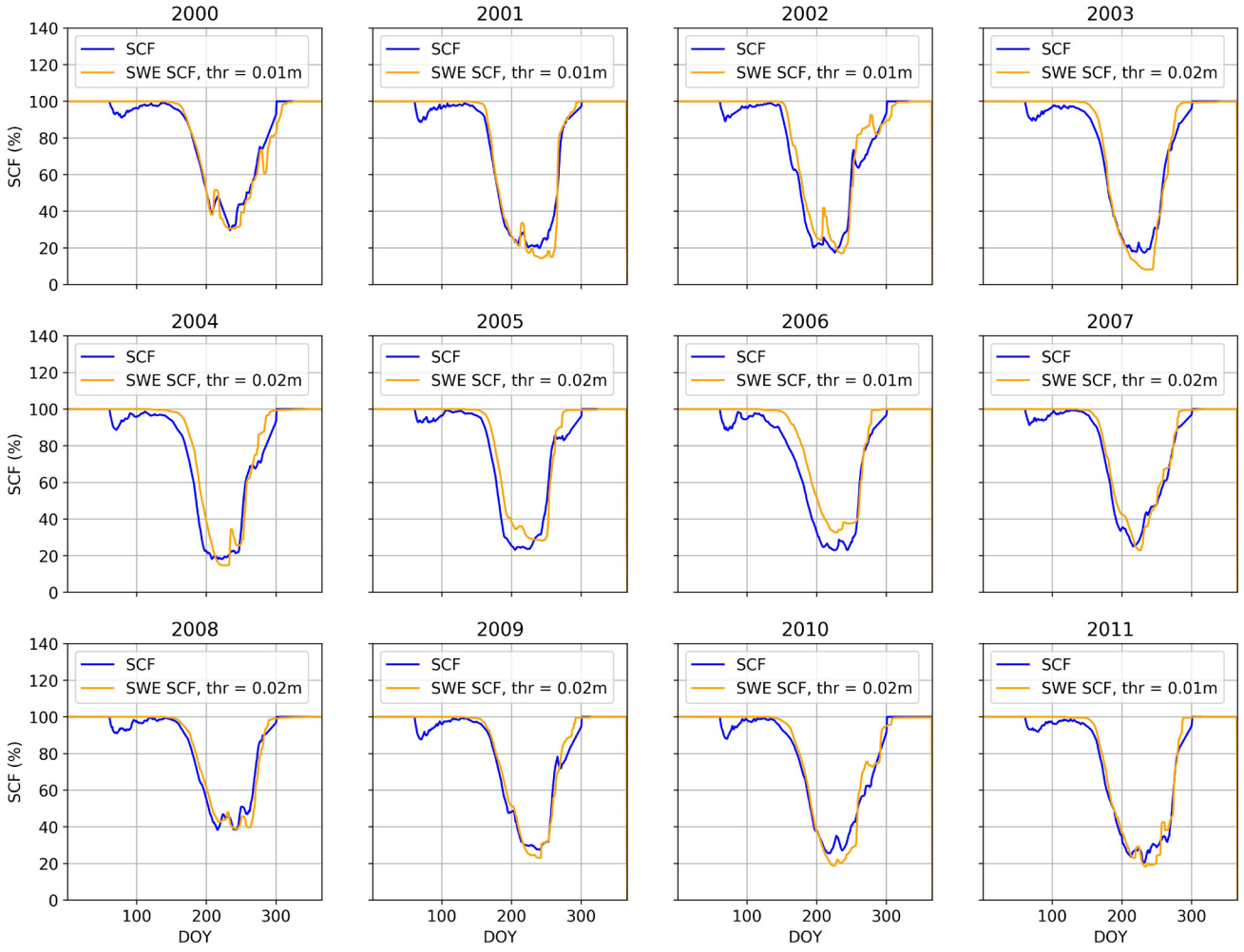

Figure 4: Comparison of SCF time series from thresholding of the older UU snow model SWE data and MODIS for all years with overlapping data (2000–2011 inclusive). The SWE thresholds producing best agreement with the MODIS data are given in the legends. The best agreement was determined by minimizing the squared differences over the yearly time series.

When SWE (UU) datasets underwent thresholding to estimate SCF, a somewhat closer agreement with the MODIS land-averaged SCF was obtained, indicated by the time series comparisons in Figure 4 and the scatter plots (Figure 5) with a positive bias in the SWE-derived SCF of approximately 10 % when MODIS SCF was >40 %. Below these values, the relationship was less linear, and the fitted spline curve suggests that MODIS estimates were on average greater than those derived from SWE. For first snow-free day estimates using MODIS and SWE SCF (Figure 6) the correlation was rather weak and MODIS estimates were generally earlier than those obtained using the SCF time series derived from SWE datasets. Interestingly in Figure 7, there was very good agreement for the estimates of the last snow free day obtained using both the MODIS and SWE-derived SCF time series. Figure 7 also shows that the strongest correlation was obtained for last snow free day using the SCF time series derived from the older SWE dataset ('SnowModel-1').

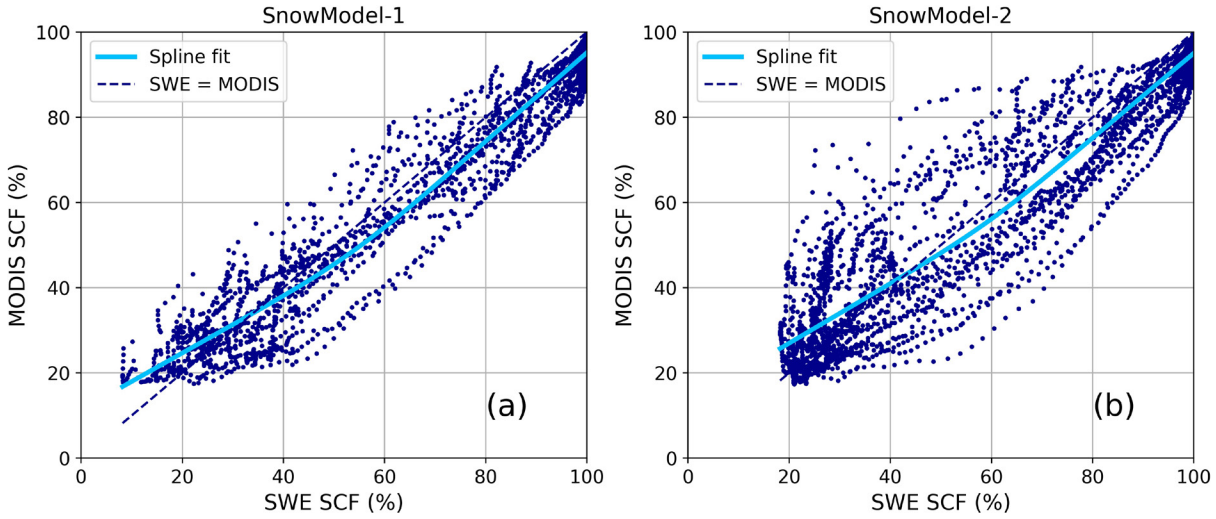

Figure 5: (**a**) Comparison of SCF from thresholding the older UU snow model SWE maps (SnowModel-1) and MODIS as a scatter plot, combining the land-averaged estimates from all DOY and all years (2000–2011). A fitted spline curve is shown in light blue. (**b**) same as for Figure 5a but using the newer UU SWE dataset for 2000–2017 inclusive (SnowModel-2).

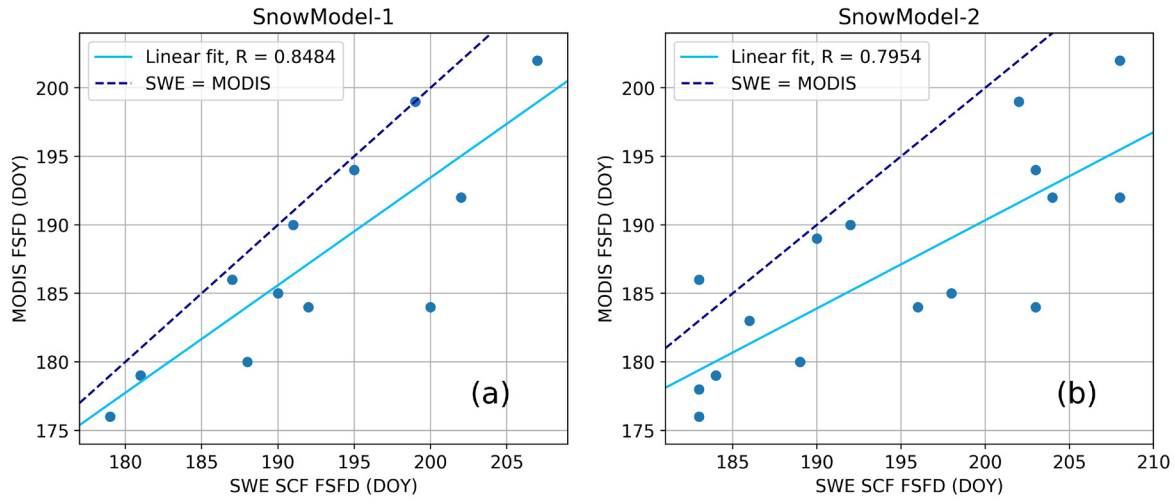

Figure 6: (**a**): Comparison of the first snow free day (FSFD) derived using the older UU snow model SWE (SnowModel-1) derived land-averaged SCF time series and the MODIS first snow free day derived from the land-averaged SCF time series. (**b**) same as for Figure 6a but using the newer UU snow model SWE dataset (SnowModel-2). In both figures, a dashed line indicates where FSFD would be the same in both datasets, while a light blue solid line shows the linear fit. Correlation coefficient R is stated in the legend.

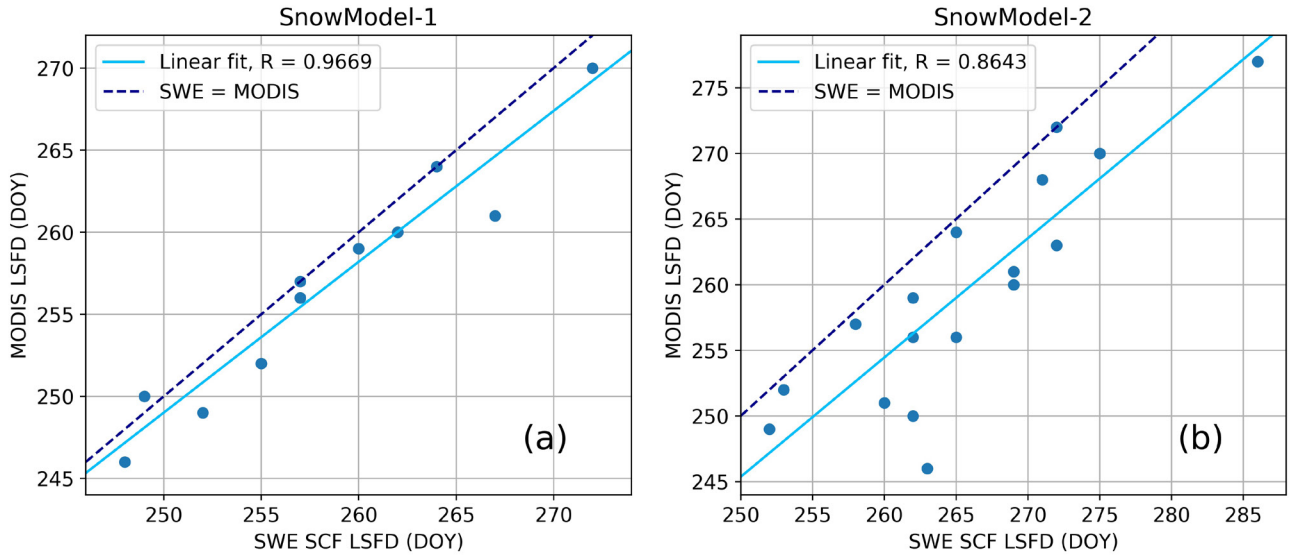

Figure 7: (**a**): Comparison of the last snow free day (LSFD) using the older UU snow model SWE (SnowModel-1) derived land-averaged SCF time series and the MODIS last snow free day derived from the land-averaged SCF time series. (**b**) same as for Figure 7a but comparing last snow free day using the newer UU snow model SWE snow model dataset (SnowModel-2). As for Figure 6, a light blue solid line indicates the linear fit to the two datasets and the dashed line shows where the LSFD from both datasets would be equal.

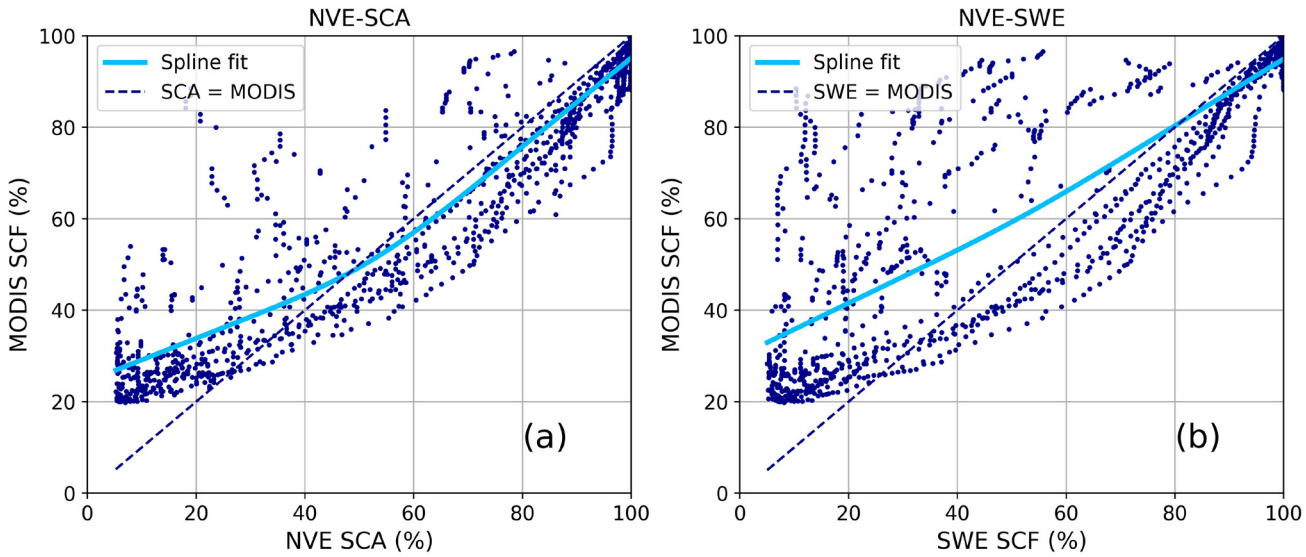

Figure 8: (**a**) Same as for Figure 5 but showing snow covered area from NVE (2013–2019) and (**b**) derived from thresholding of the NVE SWE dataset. A spline fit is shown by the light blue curve while a dashed line indicates where the two estimates would be equal.

In the case of the NVE seNorge SCA and SWE datasets, the seNorge SCA was generally lower than that obtained using the MODIS dataset for minimum snow cover during the summer months, but the degree of underestimation with respect to the MODIS dataset was greater when the SWE-derived snow cover fraction was compared. Figures 7a and 7b show the general relationship between seNorge (SWE-derived SCF) and MODIS SCF and between seNorge SCA and MODIS SCF respectively, which illustrate the underestimation of seNorge with respect to MODIS for lower snow cover fraction. For SCF > 50%, the fitted spline curve in Figure 8b shows that the MODIS SCF is on average slightly lower than that obtained from theseNorge product. Qualitatively, there was better agreement between the seNorge and MODIS time series during the first part of the year when SCF decreases toward minimum; after minimum there is less agreement leading to a lack of correlation between estimates of the last snow free day obtained from MODIS and seNorge (not shown).

For first snow free day (Figure 9), there is a more obvious linear relationship but the correlation is not particularly high and relatively similar when correlating the first snow free day derived from both SCA and thresholded SWE time series (R = 0.72 and 0.79 respectively).

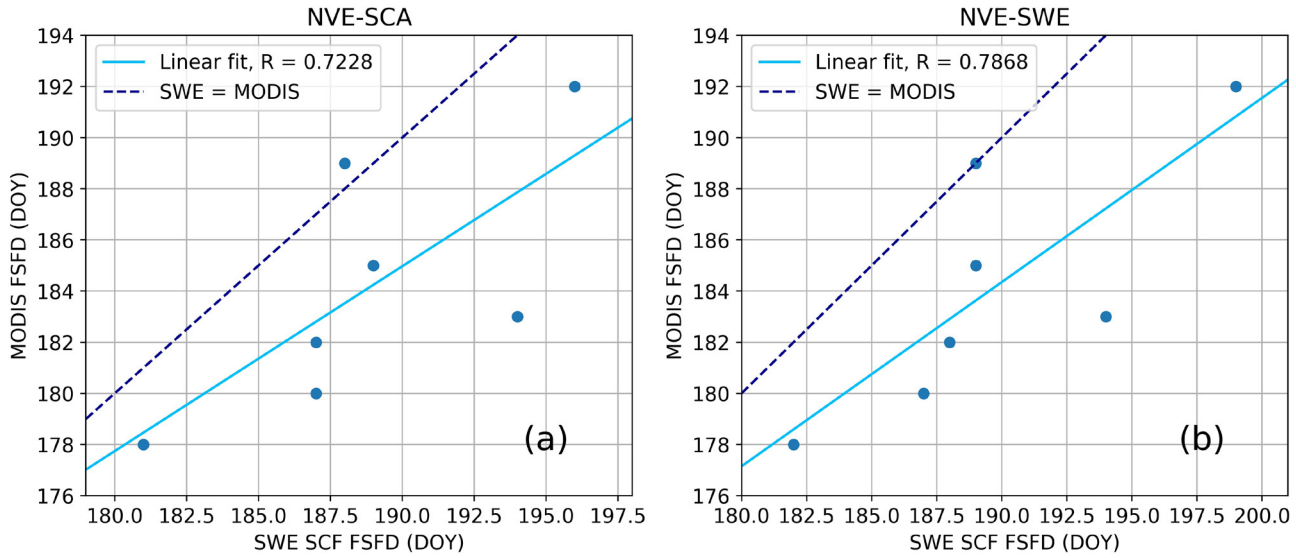

Figure 9: (**a**) Comparison of the first snow free day from MODIS and those derived using the seNorge land-averaged SCA time series and (**b**) thresholded SWE (seNorge) land-averaged SCF time series. As for Figures 5 and 6, a light blue solid line indicates the linear fit to the two datasets and the dashed line shows where the LSFD from both datasets would be equal.

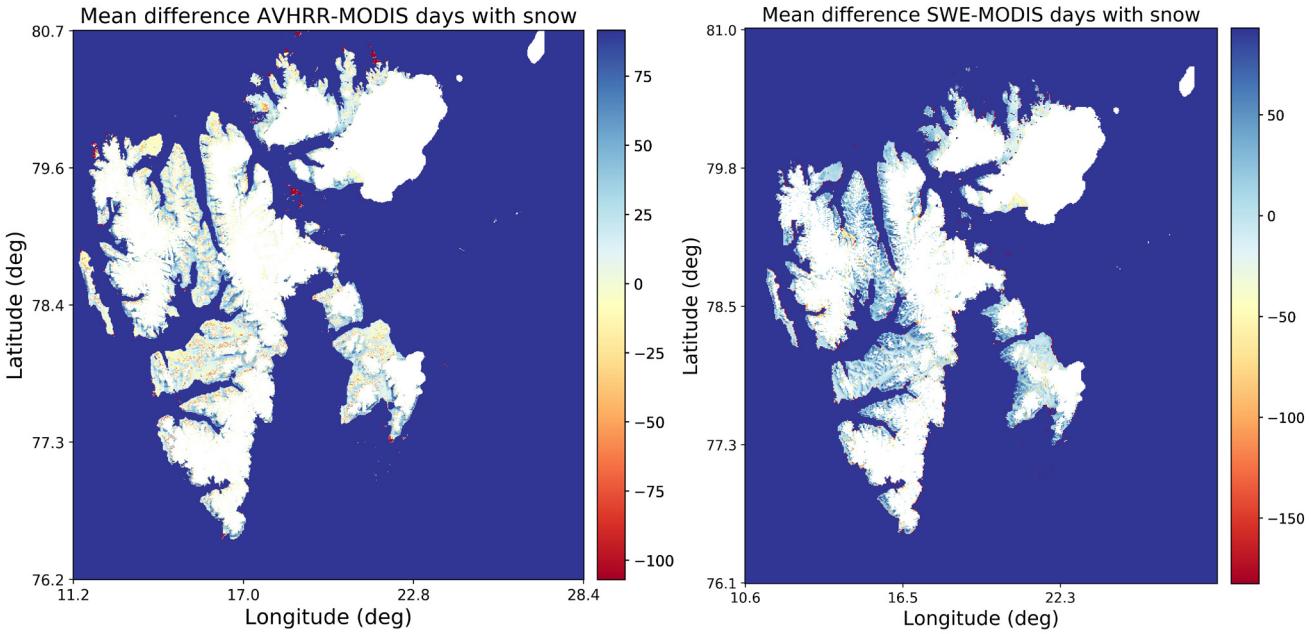

Figure 10: **a** (left) Average difference in number of days with snow cover over Svalbard for 2000–2015, comparing AVHRR SCE with MODIS SCF. The MODIS SCF has undergone thresholding at 50% to obtain a binary SCE map and **b** (right) same as for Figure 10a but using SCE derived from the older UU snow model SWE dataset (2000–2011).

For the average differences in number of days with snow cover per year estimated by AVHRR and MODIS, Figure 10a indicates that no clear regional differences are present, but qualitatively, the differences are more altitude dependent. Figure 10a shows that the mean difference between AVHRR and MODIS is primarily positive in the valleys and around the coast while at mid- and higher elevations the difference is increasingly negative, i.e., AVHRR tends to estimate more days with snow per year compared with MODIS in the low-lying areas while at higher elevations, there is an apparent underestimation of snow cover in mountainous areas. Considering the geographical distribution of the mean difference in number of days with snow cover from the UU SWE datasets (Figure 10b), there is a tendency toward positive differences across most of the archipelago i.e., the number of days with snow cover from thresholding the 1 km resolution SWE maps, is mostly greater than the number of days of snow estimated by thresholding the 500 m resolution MODIS SCF maps.

This altitude dependency exhibited in Figure 10a is largely confirmed by Figure 11, which shows the mean difference distributed in bins of 100 m from 0 to 1600 m. At the lowest altitudes of up to 200 m.a.s.l, the bin averages are around 13 days, while for the highest altitude bin at 1500–1600 m.a.s.l the bin average is of the order of –10 days i.e., AVHRR estimates on average 10 days per year less snow cover compared to MODIS in this height range. There also exist dark red regions and islands around Nordaustlandet, which represent areas not mapped by the AVHRR dataset, resulting from the resolution difference between MODIS and AVHRR. The difference is therefore large and negative since there is no snow cover data here using AVHRR. For the UU SWE dataset, an almost opposite altitudinal pattern to that for the AVHRR data was obtained (not shown); at lower elevations of up to 200 m.a.s.l, there are on average fewer days with snow cover estimated from thresholding the SWE data when compared with the MODIS dataset, while at higher elevations the SWE dataset tends to estimate more days with snow each year compared with the MODIS SCF data. In the elevation band 700–900 m.a.s.l the thresholded SWE dataset estimates on average around 30 more days with snow cover per year when compared with MODIS at these altitudes.

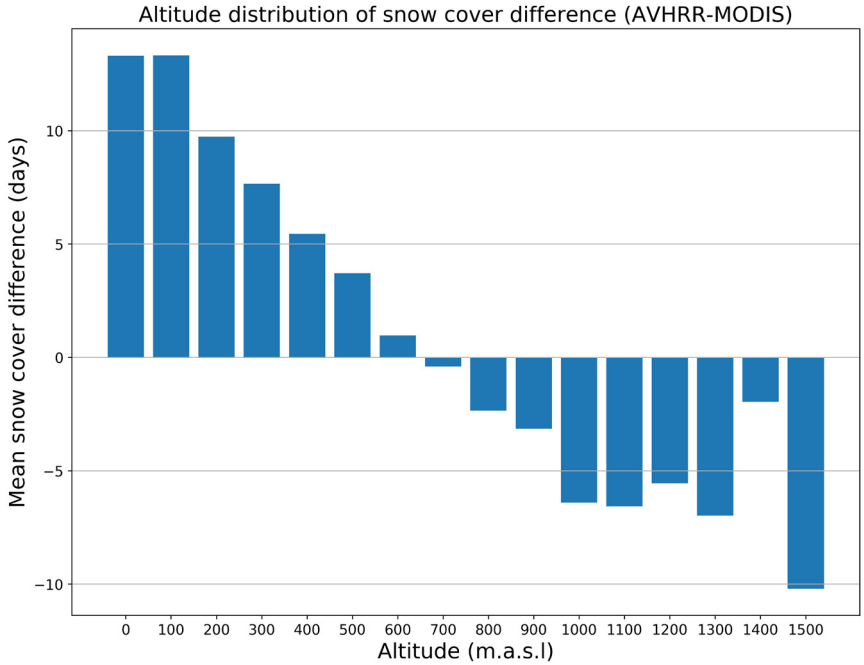

Figure 11: Altitude distribution of the mean difference in number of days with snow cover (cf. Figure 10a) comparing snow cover maps from AVHRR and MODIS for the period of 2000–2015. This figure shows clearly that the differences are positive at low altitudes (< 700 m.a.s.l.) while at higher altitudes (>800 m.a.s.l.) the mean difference in days with snow cover is negative, indicating that AVHRR overestimates the number of days with snow with respect to MODIS at low altitudes, while at high altitudes AVHRR underestimates number of days with snow with respect to MODIS. Best agreement for number of days with snow is found at altitudes between 700–800 m.a.s.l.

For the Sentinel 2–MODIS comparison, Figure 1 shows an example of the snow cover fraction maps for a part of Nordenskiöld Land in central Svalbard for 7th June 2018. Qualitatively, some differences can be observed as the S2 SCF map exhibits smaller variation in the range of SCF than the MODIS map. This may be explained by the large difference in spatial resolution between the two sensors, whereby MODIS tends to smooth out snow cover with intermediate snow cover fractions to a greater extent than S2. Since S2 only is available for two years during the SATMODSNOW project, a thorough intercomparison between the two datasets has not been performed here. With ongoing acquisition of further data from S2 it is hoped that within a few years, a larger database will allow a more in-depth comparison of SCF estimated by the two sensors, qualitatively and quantitatively.

4. Connections and synergies with other SESS report chapters

4.1. This year

Killie et al. (2021): 'Svalbard long-term variabilities of terrestrial-snow and sea-ice cover extent'. There are clear synergies between this and the current study. In the case of comparing terrestrial snow and sea-ice cover, a parallel study using the MODIS snow cover dataset was carried out by Vickers et al. (2020), which is a pre-cursor to the current SESS project.

Salzano R. et al. (2021): 'Terrestrial Photography Applications on Snow cover in Svalbard'. The methods used by Salzano should have synergies when validating satellite data. In particular, it could be interesting to translate the long-term time series of webcam data on the Zeppelin mountain into a georeferenced snow cover dataset, perhaps used as a long-term reference dataset to quantify differences in SCF estimates using different sensors with variable spatial resolution.

4.2. Previous years

Karlsen et al. (2020): 'Sentinel based mapping of plant productivity in relation to snow duration and time of green-up'. This report focuses on in-situ and satellite data from the Adventdalen region linked to plant productivity measurements. Current high-resolution Sentinel-1&2 sensors are well suited to accurately map the plant phenology and determine plant productivity. There are obvious synergies between the datasets used in Karlsen et al. (2019) and in this study, and the S2 dataset used is simply a by-product of the S2 NDVI dataset used. Synergies by combining various snow products are shown in the current report and could be extended to plant productivity.

Gallet et al. (2019): 'Snow research in Svalbard: current status and knowledge gaps. The authors provide an overview of current snow research on Svalbard and identify needs for further research within the three main fields: glacial snow, seasonal snow on land and impacts of contaminants in snow. Based on the recommendations in this report (specifically related to seasonal snow on land), we believe that the SATMODSNOW project has at least partially provided answers to these recommendations by promoting scientific exchanges of data and interdisciplinary work (remote sensing/hydrology).

5. Unanswered questions

While this review has been able to address the first two objectives (outlined in section 1), as summarized in section 4, the third objective has only been answered to a certain extent in terms of suggesting potential methods to improve low resolution datasets (e.g. AVHRR) using higher-resolution datasets (e.g. MODIS or S2). In the results, the relationships between MODIS datasets and the AVHRR and snow model products are described. The remote sensing comparisons suggest that lower resolution sensors tend to overestimate SCF with respect to the higher resolution sensors (e.g. AVHRR-MODIS, MODIS-Sentinel 2 comparisons). This overestimation can be up to several tens of per cents. However, due to the Sentinel-2 dataset in this analysis being comparatively small in terms of temporal (two seasons) and spatial coverage, further analysis is required to fully establish the correction required to improve the lower resolution MODIS dataset. Acquiring additional Sentinel-2 scenes covering a greater area of Svalbard over the forthcoming years would contribute greatly to the understanding of the differences in SCF obtained at high and moderate spatial resolutions. Once this is ascertained, a corrected MODIS dataset should be used to update the regression obtained with the AVHRR dataset, thereby propagating the corrections down to the lowest sensor resolutions and allowing a long time series of SCF to be reconstructed at high spatial resolution. The potential of fusing models for SWE with satellite observations of snow cover is also high and should be used for improving models in the future. Various approaches could be envisioned for obtaining more realistic snow distributions but finding an acceptable compromise between the satellite observations and the input fields (mainly temperature and precipitation) used in the hydrological models is crucial.

6. Recommendations for the future

- The results in SATMODSNOW and other snow services such as CCI Snow should be utilized to compile a long-term time series of snow cover data for 1978–2020 with as high spatial resolution as possible. Such a consolidated dataset could play an important role in future snow research on Svalbard as well as interdisciplinary research within e.g. ecology, geophysics and climate research.

- Future efforts to integrate multi-source EO data (in situ, airborne and satellite observations) with new techniques (e.g. artificial intelligence and data assimilation) are highly recommended for further improving the characterization of snow cover and SWE in Svalbard.

- Methods to utilize EO data to improve hydrological models should be sought in order to better capture the snow cover distribution simultaneously as SWE estimates are improved.

- The snow measurement infrastructure on Svalbard needs improvements for providing more validation/ground truthing for both models and EO datasets. In addition to traditional ground instruments (met-stations, snow field surveys), datasets providing spatial coverage such as air- or UAV-borne are also needed, among others to reveal more details on the spatial snow distribution. Sensors that can measure additional snow properties such as temperature and liquid water content are also of interest.

- Upcoming datasets from EO (e.g. wet snow from SAR) should be compared and validated using corresponding layers from hydrological modelling (e.g. liquid water content) in the future.

7. Data availability

Table 1: Overview of all the data used in the project, and the availability of the datasets.

Dataset	Parameters	Period	Location or area	Metadata / Data access (URL, DOI)	Data provider, reference
MODIS	Snow cover fraction	2000–2020	Svalbard	Available in the SIOS data access portal in Q1 2021 https://doi.org/10.3390/rs12071123	NORCE
AVHRR	Snow probability	1982–2015	Svalbard	SIOS database; the URL will be added before the SESS report will be published	METNO
Sentinel-2	Snow cover fraction	2017–2020	Nordenskiöld Land	-	NORCE skar@norceresearch.no
SeNorge	Snow water equivalent, Snow covered area	2012–2019	Svalbard	www.senorge.no	NVE, tus@nve.no
SnowModel	Snow water equivalent	2000–2011 and 1957–2018	Svalbard	SIOS data access portal: https://bit.ly/3nkfu18	Uppsala University (UU), ward.van.pelt@geo.uu.se

Table 2: Datasets overview showing a comparison of the remote sensing datasets (Sentinel-2, MODIS, AVHRR) and SWE datasets derived from snow models (seNorge, UU) in terms of the time period with data coverage, spatial resolution, snow cover variables and if the polar night period is available.

	Sentinel2	MODIS	AVHRR	SeNorge	UU
Time-period	2016-	2000–2020	1982–2015	2012–2019	2000–2011(old) 1957–2018(new)
Spatial resolution	20 m	500m	4km	1km	1km
Wavelengths used	510–580 nm 860–1040 nm	545–565 nm 1628–1652 nm	580–680 nm 3550–3930 nm	N/A	N/A
Snow extent	Snow cover fraction	Snow cover fraction	Snow probability	Separate SCF layer or derived from SWE using 1 cm threshold	Derived from SWE using 1 cm threshold, (2 cm in 2003/2004)
Snow mass	N/A	N/A	N/A	SWE/snow depth	SWE
Polar night	N/A	N/A	N/A	Yes	Yes

Acknowledgements

This work was supported by the Research Council of Norway, project number 251658, Svalbard Integrated Arctic Earth Observing System – Knowledge Centre (SIOS-KC).

List of abbreviations

AVHRR	Advanced Very High Resolution Radiometer
EO	Earth Observation
FSFD/LSFD	First/Last Snow Free Day
MODIS	Moderate Resolution Imaging Spectroradiometer
NDSI/NDVI	Normalized Differential Snow/Vegetation Index
NVE	The Norwegian Water Resources and Energy Directorate
NWP	Numerical weather prediction model
S2	Sentinel-2
SCE	Snow Cover Extent
SCF/SCA	Snow Cover Fraction/Snow Covered Area
SWE	Snow Water Equivalent
UU	Uppsala University

References

Eckerstorfer M, Malnes E, Christiansen HH (2017) Freeze/thaw conditions at periglacial landforms in Kapp Linné, Svalbard, investigated using field observations, in situ, and radar satellite monitoring. Geomorphology 293:433–447.

Gallet JC, Björkman MP, Borstad CP, Hodson AJ, Jakobi H-W, Larose C, Luks B, Spolaor A, Schuler TV, Urazgildeeva A, Zdanowicz C (2019) Snow research in Svalbard: current status and knowledge gaps. In: Orr et al. (eds): SESS report 2018.Svalbard Integrated Arctic Earth Observing System, Longyearbyen, pp 83–107 . https://sios-svalbard.org/SESS_Issue1

Gascoin S, Grizonnet M, Bouchet M, Salgues G, Hagolle O (2019) Theia Snow collection: High-resolution operational snow cover maps from Sentinel-2 and Landsat-8 data. Earth Syst Sci Data 11(2).

Hall DK, Riggs GA, Salomonson VV, DiGirolamo NE, Bayr KJ (2002) MODIS snow-cover products. Remote Sens Environ 83:181–194.

Karlsson KG, Anttila K, Trentmann J, Stengel M, Fokke Meirink J, Devasthale A, Hanschmann T, Kothe S, Jääskeläinen E, Sedlar J, Benas N, van Zadelhoff GJ, Schlundt C, Stein D, Finkensieper S, Håkansson N, Hollmann R (2017) CLARA-A2: the second edition of the CM SAF cloud and radiation data record from 34 years of global AVHRR data. Atmos Chem Phys 17:5809–5828.

Karlsen SR, Stendardi L, Nilsen L, Malnes E, Eklundh L, Julitta T, Burkart A, Tømmervik H (2020) Sentinel satellite-based mapping of plant productivity in relation to snow duration and time of green-up (GROWTH). In: Van den Heuvel et al. (eds): SESS report 2019.Svalbard Integrated Arctic Earth Observing System, Longyearbyen, pp 43–57 . https://sios-svalbard.org/SESS_Issue2

Killie MA (2018) Validation of a satellite-based Snow Cover Index for Svalbard, SIOS Access project 2018_0007

Killie MA, Aaboe S, Isaksen K, Van Pelt W, Pedersen ÅØ, Luks B (2021) Svalbard snow and sea-ice cover: comparing satellite data, on-site measurements, and modelling results. In: Ibáñez et al (eds) 2021: SESS report 2020, Svalbard Integrated Arctic Earth Observing System, Longyearbyen, pp 220-235. https://doi.org/10.5281/zenodo.4293804

Malnes E, Karlsen SR, Johansen B, Haarpaintner J, Hogda KA (2010) Monitoring of the snow coverage and its relation to vegetation and growing seasons on Svalbard using ENVISAT ASAR and TERRA MODIS data. ESASP 686:265.

Nagler T, Rott H (2000) Retrieval of wet snow by means of multitemporal SAR data. IEEE Trans Geosci Remote Sens 38:754–765.

Pulliainen J, Luojus K, Derksen C, Mudryk L, Lemmetyinen J, Salminen M, Ikonen J, Takala M, Cohen J, Smolander T, Norberg J, J (2020) Patterns and trends of Northern Hemisphere snow mass from 1980 to 2018. Nature 581(7808):294–298.

Rotschky G, Vikhamar Schuler T, Haarpaintner J, Kohler J, Isaksson E (2011) Spatio-temporal variability of snowmelt across Svalbard during the period 2000–08 derived from QuikSCAT/SeaWinds scatterometry. Polar Res 30(1):5963.

Saloranta TM (2012) Simulating snow maps for Norway: description and statistical evaluation of the seNorge snow model. The Cryosphere 6(6):1323.

Saloranta TM (2014) New version (v.1.1.1) of the seNorge snow model and snow maps for Norway, Rapport 6-2014, Norwegian Water Resources and Energy Directorate, Oslo, Norway, p 30. Available at http://publikasjoner.nve.no/rapport/2014/rapport2014_06.pdf

Saloranta TM (2016) Operational snow mapping with simplified data assimilation using the seNorge snow model. J Hydrol 538:314–325.

Salzano R, Aalstad K, Boldrini E, Gallet JC, Kępski D, Luks B, Nilsen L, Salvatori R, Westermann S (2021 a) Terrestrial photography applications on snow cover in Svalbard. In: Moreno-Ibáñez et al (eds) SESS report 2020, Svalbard Integrated Arctic Earth Observing System, Longyearbyen, pp 236-251. https://doi.org/10.5281/zenodo.4294084

Sentinel-2 User guide: https://sentinel.esa.int/web/sentinel/user-guides/sentinel-2-msi

Stendardi L (2020) Detection of vegetation phenology in cold regions using a combination of radar and optical satellite data. PhD Thesis, University of Bolzano/Bozen (Italy)

Van Pelt WJJ, Oerlemans J, Reijmer CH, Pohjola VA, Pettersson R, van Angelen JH (2012) Simulating melt, runoff and refreezing on Nordenskiöldbreen, Svalbard, using a coupled snow and energy balance model. The Cryosphere 6:641–659.

Van Pelt WJ, Kohler J, Liston GE, Hagen JO, Luks B, Reijmer CH, Pohjola VA (2016) Multidecadal climate and seasonal snow conditions in Svalbard. J Geophys Res: Earth Surface 121(11):2100–2117.

Van Pelt WJJ, Pohjola VA, Pettersson R, Marchenko S, Kohler J, Luks B, Hagen JO, Schuler TV, Dunse T, Noël B, Reijmer CH (2019) A long-term dataset of climatic mass balance, snow conditions and runoff in Svalbard (1957–2018). The Cryosphere 13:2259–2280.

Vickers H, Karlsen SR, Malnes E (2020) A 20-Year MODIS-Based Snow Cover Dataset for Svalbard and Its Link to Phenological Timing and Sea Ice Variability. Remote Sens 12(7):1123.